THREE-DIMENSIONAL STABILITY ANALYSIS OF A UNIAXIALLY COMPRESSED POLYNOMIALLY THICK RECTANGULAR PLATES USING ENERGY METHOD

Onyeka F C.[1, 3], Nwa-David C D.[2] and Okeke T E.[3],*

[1]Department of Civil Engineering, Edo State University Uzairue, Edo State.
[2]Department of Civil Engineering, University of Nigeria, Nsukka.
[3]Department of Civil Engineering, Michael Okpara University of Agriculture, Umudike.

Abstract

This study presents the three-dimensional (3-D) stability analysis of a uniaxially compressed thick rectangular isotropic plate that is clamped in one edge and the other three edges simply supported (CSSS). The energy method was applied in the coupling the three dimensional kinematics and constitutive relations to formulate the total potential energy equation. The formulated the total potential energy for the plate was transformed into equilibrium equation and used to obtain the shape function of the plate. The shape function derived was analysed through variational principle to get an exact polynomial displacement function which is a product of the coefficient of deflection and shape function of the plate. The expression for the critical buckling load and other formulae was obtained by the direct variation of the total potential energy equation to produce a reliable solution for stability analysis of any type of plate rectangular plate. The span to thickness ratio and aspect ratios were varied to ascertain the buckling behavior of different type of plate under uniformly distributed load. The outcome of the numerical analysis revealed that increase in the span-thickness ratio led to the increased value of the critical buckling load which implies that the plate structure is safe when the plate thickness is increased. The result showed that the critical buckling loads from the present study using the established 3-D model for both functions is satisfactory and were found to follow an identical pattern, but quite distinct in validation which shows the credibility of the derived relationships. The overall average percentage differences between the two functions recorded are 2.06%. This shows that at about 98% both approaches are the same and can be applied with confidence in the stability analysis of any type of plate with such boundary condition.

Keywords: CSSS rectangular plate, stability analysis 3-D plate, exact polynomial function, critical buckling load.

1. Introduction

Plates which are basically three-dimensional structural elements whose straight and plane surfaces are geometrically large compared to its thickness [1, 2, 3]; have attracted much research interest among scholars due to its extensive applications in mechanical, aerospace, aeronautics and structural engineering [4, 5]. Plate materials are often used in structural engineering as ship hull and spacecraft, bridge deck, building slabs, and retaining wall for water retaining structures [6, 7].

Plates can be homogeneous, laminated, or functionally graded with different sizes, thicknesses and shapes depending on their applications as it varies. Plates can be clamped, simply supported or have free boundary conditions. With respect to shapes, plates can be skewed, elliptical, triangular, square, circular, or rectangular, also they can be anisotropic and isotropic plates, based on material composition. Based on depth, plates can be thin, thick or moderately thick [8]. Rectangular plates with $50 \leq a/t \leq 100$ were considered as thin plate, $20 \leq a/t \leq 50$ as moderately thick and $a/t \leq 20$ as thick plate where a/t is the span-to-depth ratio [9].

The relevance of thick plates in the construction industry has greatly increased and has drawn the attention of researchers for more investigation, because of their advantages such as its load resistance ability, light weight and high strength [10].

Corresponding Author**:** Onyeka F.C., Email: onyekachuks@gmail.com, Tel: +2348068285789

These investigations consist of vibration, bending and buckling [11, 12]. Instability is commonly seen through buckling and plate buckles or becomes unstable due to in-plane loading [13]. The extent to which plates experience instability because of in-plane compressive forces is called the critical buckling load [14]. When the in-plane loading exceeds the critical value, plate's encounters large deformations and total failure may occur. The essence of buckling analysis is to determine the critical buckling load of the plate. More and accurate method of analysis is needed in order to overcome plate failure.

To solve the problem of instability due to buckling, several theories such as the classical plate theory (CPT) [15], and the refined plate theories (RPT) have been developed by different scholars. CPT is usually used in the thin plate analysis as it is based on the assumptions of Kirchhoff [16]. Unlike CPT, in RPT the shear deformation effect is considered. These refined plate theories include; the first order shear deformation theory (FSDT) [17] and the higher-order shear deformation plate theory (HSDT) [18]. In contrast to FSDT, HSDT does not require a correction factor to produce satisfactory results. However, these HSDTs cannot yield accurate solutions for a typical 3-D plate. The 3-D plate theory is required in order to obtain an exact solution for a three-dimensional plate during stability analysis. And this validates the significance of this study.

The stability study can be carried out using either equilibrium, numerical, energy methods or a combination of any [19]. Numerical methods such as finite difference methods, boundary element methods, and truncated double Fourier series, often yields approximate solutions of the plate problem. To obtain exact solution it requires so much time and lots of work. Energy method differs from numerical and the equilibrium method in that it adds all the strain energy and potential energy or external work on the continuum to be equal to the total potential energy [20, 21]. This work is based on energy method.

Using the virtual work principle based on polynomial shape function, the author in [22] developed a model to obtain the buckling coefficients for stiffened rectangular plates. Thick plate was not part of their consideration as their assumption was limited to the CPT. But, the author in [12] employed 2-D theory with an energy method to analyze the buckling behavior of thick plates. To obtain the total potential energy which was reduced to the governing equation, the authors combined the strain energy and external work. The authors neglected all the stress and strain along the thickness direction of the plate and failed to address CSSS plates in their analysis.

Authors in [23] and [24] studied thick plates subjected to biaxial and uniaxial in-plane forces, using RPT to obtain the buckling solution. The authors in [24] used the virtual work principle and applied a 2-D plate theory to investigate the buckling of simply supported isotropic rectangular plate. A typical 3-D thick plate with CSSS boundary conditions were not considered by both authors and polynomial displacement functions were not taken into account.

In [25], the authors applied 2-D theories to investigate the stability of elastic thick plates. Their study did not consider the stresses in the direction of thickness axis. The outcome of their analysis was not a close-form solution as the shape function used were assumed. The authors failed to cover plates with CSSS boundary conditions.

The authors in [26] employed displacement potential function method and used an assumed shape function to obtain the solution of buckling of thick plates that are simply supported. The authors applied method of variable separation and satisfied the support conditions of the plate in order to establish the governing differential equations. The authors did not use displacement function that stems from the compatibility equation, and their study did not cover CSSS plates.

In [27], the authors employed direct variational calculus to analyze the stability of clamped at the three edge and the other remaining edge simply supported (CCCS) rectangular plates, considering polynomial displacement functions they establish a new model for analyzing the buckling of thick plates. From 3-D constitutive relations, the authors formulated the governing equation of the plate which when solved give equation for the analysis. Their analysis failed to cover CSSS plate. The authors in [28] covered CSSS boundary conditions in their thick plates buckling analysis and the outcome of their study was satisfactory as their result were closer to exact solution compared to 2-D theories. But they failed to apply polynomial shape functions which is easier to apply especially for a complicated boundary condition like 3-D CSSS support.

From previous studies, it can be observed that many researchers have applied CPT and several 2-D theories while very few scholars have considered the 3-D plate theory for buckling analysis of plates. The distinctiveness of this present study over the previous works lies in the displacement function used, the plate boundary condition, the plate theory and the method of analysis. In this study, the variational energy method is applied to formulate and derive a three-dimensional plate theory (3-D) for stability analysis of thick isotropic plates elastically restrained along one edge and other three edges simply supported (CSSS) under uniaxial compressive load, using polynomial shape functions. The shape function was derived from equilibrium equation after the energy equation transforming through variational principle to get an exact polynomial displacement function which produce a reliable solution for stability analysis of any type of plate rectangular plate.

2. Theoretical Analysis

A three dimensional kinematics and constitutive relations was used to obtain the equation of total energy functional based on the static elastic theory of plate. The stress-strain relationship for an isotropic material under elastic condition as described using generalized Hooke's law is given as:

$$\begin{bmatrix} \varepsilon_x \\ \varepsilon_y \\ \varepsilon_z \\ \gamma_{xz} \\ \gamma_{yz} \\ \gamma_{xy} \end{bmatrix} = \frac{1}{E} \begin{bmatrix} 1 & -\mu & -\mu & 0 & 0 & 0 \\ -\mu & 1 & -\mu & 0 & 0 & 0 \\ -\mu & -\mu & 1 & 0 & 0 & 0 \\ 0 & 0 & 0 & 2(1+\mu) & 0 & 0 \\ 0 & 0 & 0 & 0 & 2(1+\mu) & 0 \\ 0 & 0 & 0 & 0 & 0 & 2(1+\mu) \end{bmatrix} \begin{bmatrix} \sigma_x \\ \sigma_y \\ \sigma_z \\ \tau_{xz} \\ \tau_{yz} \\ \tau_{xy} \end{bmatrix} \tag{1}$$

Where:
Modulus of elasticity and Poisson's ratios are denoted with E and μ respectively, the symbol ε_x denotes normal strain along x axis, the symbol ε_y denotes normal strain along y axis, the symbol ε_z denotes normal strain along z axis, the symbol γ_{xy} denotes shear strain in the plane parallel to the x-y plane, the symbol γ_{xz} denotes shear strain in the plane parallel to the x-z plane, the symbol γ_{yz} denotes shear strain in the plane parallel to the y-z plane.
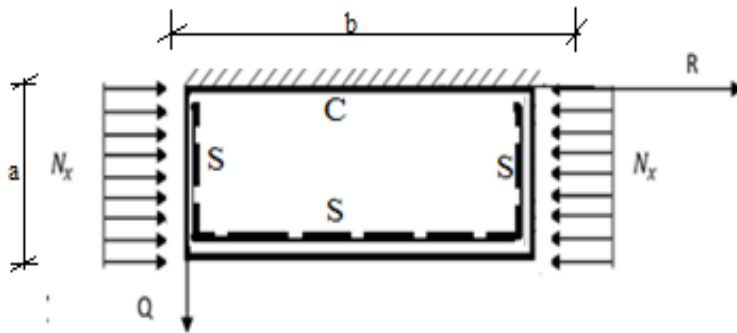

Figure 1: CSSS rectangular plate subjected to a uniaxial compressive load
From the Figure 1, the non-dimensional form of coordinates is given as: R = x/a, Q = y/b and S = z/t corresponding to x, y and z-axes respectively. The spatial dimensions of the plate along x, y and z-axes are a, b and t respectively, as the t is the thickness of the plate, thus the six strain components is obtained using the established Hooke's law as:

$$\varepsilon_x = \frac{St}{a}\frac{d\theta_x}{dR} \tag{2}$$

$$\varepsilon_y = \frac{St}{a\beta}\frac{d\theta_y}{dQ} \tag{3}$$

$$\varepsilon_z = \frac{1}{t}\frac{dw}{dS} \tag{4}$$

$$\gamma_{xy} = \frac{St}{a\beta}\frac{d\theta_x}{dQ} + \frac{St}{a}\frac{d\theta_y}{dR} \tag{5}$$

$$\gamma_{xz} = \theta_x + \frac{1}{a}\frac{dw}{dR} \tag{6}$$

$$\gamma_{yz} = \theta_y + \frac{1}{a\beta}\frac{dw}{dQ} \tag{7}$$

Similarly the six stress components gives:

$$\sigma_x = \frac{Ets}{(1+\mu)(1-2\mu)a}\left[(1-\mu)\cdot\frac{\partial\theta_x}{\partial R} + \frac{\mu}{\beta}\cdot\frac{\partial\theta_y}{\partial Q} + \frac{\mu a}{st^2}\cdot\frac{\partial w}{\partial S}\right] \tag{8}$$

$$\sigma_y = \frac{Ets}{(1+\mu)(1-2\mu)a}\left[\mu\cdot\frac{\partial\theta_x}{\partial R} + \frac{(1-\mu)}{\beta}\cdot\frac{\partial\theta_y}{\partial Q} + \frac{\mu a}{st^2}\cdot\frac{\partial w}{\partial S}\right] \tag{9}$$

$$\sigma_z = \frac{Ets}{(1+\mu)(1-2\mu)a}\left[\mu\cdot\frac{\partial\theta_x}{\partial R} + \frac{\mu}{\beta}\cdot\frac{\partial\theta_y}{\partial Q} + \frac{(1-\mu)a}{st^2}\cdot\frac{\partial w}{\partial S}\right] \tag{10}$$

$$\tau_{xy} = \frac{E(1-2\mu)ts}{2(1+\mu)(1-2\mu)a}\cdot\left[\frac{1}{\beta}\frac{\partial\theta_x}{\partial Q} + \frac{\partial\theta_y}{\partial R}\right] \tag{11}$$

$$\tau_{xz} = \frac{E(1-2\mu)ts}{2(1+\mu)(1-2\mu)a}\cdot\left[\frac{a}{ts}\theta_x + \frac{1}{ts}\frac{\partial w}{\partial R}\right] \tag{12}$$

$$\tau_{yz} = \frac{E(1-2\mu)ts}{2(1+\mu)(1-2\mu)a}\cdot\left[\frac{a}{ts}\theta_y + \frac{1}{\beta ts}\frac{\partial w}{\partial Q}\right] \tag{13}$$

2.1. Energy Equation

Total potential energy functional is the algebraic summation of strain energy and external work. This mathematically expressed as:

$$\prod = U - V \tag{14}$$

Given that the strain energy is;

$$U = \frac{abt}{2} \int_0^1 \int_0^1 \int_{-0.5}^{0.5} \left(\sigma_x \varepsilon_x + \sigma_y \varepsilon_y + \sigma_z \varepsilon_z + \tau_{xy}\gamma_{xy} + \tau_{xz}\gamma_{xz} + \tau_{yz}\gamma_{yz} \right) dR\, dQ\, dS \tag{15}$$

And the external work for buckling load is given as:

$$V = \frac{abN_x}{2a^2} \int_0^a \int_0^b \left(\frac{\partial w}{\partial R}\right)^2 dR\, dQ \tag{16}$$

Putting Equations (2) to (13) into (15) and substituting (15) and (16) into (14) gives:

$$\prod = D^* \frac{(1-\mu)ab}{2a^2(1-2\mu)} \int_0^1 \int_0^1 \left[(1-\mu)\left(\frac{\partial\theta_{sx}}{\partial R}\right)^2 + \frac{1}{\beta}\frac{\partial\theta_{sx}}{\partial R}.\frac{\partial\theta_{sy}}{\partial Q} + \frac{(1-\mu)}{\beta^2}\left(\frac{\partial\theta_{sy}}{\partial Q}\right)^2 + \frac{(1-2\mu)}{2\beta^2}\left(\frac{\partial\theta_{sx}}{\partial Q}\right)^2 + \frac{(1-2\mu)}{2}\left(\frac{\partial\theta_{sy}}{\partial R}\right)^2 \right.$$

$$+ \frac{6(1-2\mu)}{t^2}\left(a^2\theta_{sx}{}^2 + a^2\theta_{sy}{}^2 + \left(\frac{\partial w}{\partial R}\right)^2 + \frac{1}{\beta^2}\left(\frac{\partial w}{\partial Q}\right)^2 + 2a.\theta_{sx}\frac{\partial w}{\partial R} + \frac{2a.\theta_{sy}}{\beta}\frac{\partial w}{\partial Q}\right) + \frac{(1-\mu)a^2}{t^4}\left(\frac{\partial w}{\partial S}\right)^2$$

$$\left. - \frac{N_x}{D^*}.\left(\frac{\partial w}{\partial R}\right)^2 \right] \partial R \partial Q \tag{17}$$

where D is the Rigidity of the CPT or incomplete 3-D thick plate, let
$N_x, \mu, w, \theta_{Sx},$ and θ_{Sy} are the uniform applied uniaxial compression load of the plate, the poison ratio, deflection, shear deformation rotation along x axis and shear deformation rotation along y axis respectively.

2.2. Equilibrium and Governing Equation

Minimizing the energy equation in (17) with respect to rotation in x-z plane and rotation in y-z plane $\left(\theta_{Sx}, \text{and } \theta_{Sy}\right)$ and simplifying the outcome using the law of addition gives the two equations of equilibrium Equations (18) and (19) in x-z plane and y-z plane respectively:

$$\frac{\partial w}{\partial R}\left[(1-\mu)\frac{\partial^2}{\partial R^2} + \frac{1}{\beta^2}.\frac{\partial^2}{\partial Q^2}(1-\mu) + \frac{6(1-2\mu)a^2}{t^2}.\left(1+\frac{1}{c}\right)\right] = 0 \tag{18}$$

$$\frac{1}{\beta}.\frac{\partial w}{\partial Q}\left[\frac{\partial^2}{\partial R^2}(1-\mu) + \frac{(1-\mu)}{\beta^2}\frac{\partial^2}{\partial Q^2} + \frac{6(1-2\mu)a^2}{t^2}.\left(1+\frac{1}{c}\right)\right] = 0 \tag{19}$$

One of the possibilities of Equation (18) to be true is for the terms in the bracket to sum to zero. Adding terms in the brackets of Equation (18) and (19) gives:

$$\frac{6(1-2\mu)(1+c)}{t^2} = -\frac{c(1-\mu)}{a^2}\left(\frac{\partial^2}{\partial R^2} + \frac{1}{\beta^2}\frac{\partial^2}{\partial Q^2}\right) \tag{20}$$

Similarly, the general governing equation is obtained by differentiating the Energy equation with respect to deflection and simplifying the outcome by substituting Equation (20) into it to get:

$$\frac{D^*}{2a^2}\int_0^1\int_0^1\left[\frac{6(1-2\mu)(1+c)}{t^2}\left(\frac{\partial^2 w}{\partial R^2} + \frac{1}{\beta^2}.\frac{\partial^2 w}{\partial Q^2}\right) + \frac{(1-\mu)a^2}{t^4}\frac{\partial^2 w}{\partial S^2} - \frac{N_x}{D^*}.\frac{\partial^2 w}{\partial R^2}\right] dR\, dQ = 0 \tag{21}$$

That is:

$$\frac{D^*}{2a^4}\int_0^1\int_0^1\left[\left(\frac{\partial^4 w_1}{\partial R^4} + \frac{2}{\beta^2}.\frac{\partial^4 w_1}{\partial R^2\partial Q^2} + \frac{1}{\beta^4}.\frac{\partial^4 w_1}{\partial Q^4} - \frac{N_{x1}a^4}{gD^*}.\frac{\partial^2 w_1}{\partial R^2}\right)w_S + \frac{w_1}{g}\left(\frac{(1-\mu)a^4}{t^4}.\frac{\partial^2 w_S}{\partial S^2} - \frac{N_{xs}a^4}{D^*}.\frac{\partial^2 w_S}{\partial R^2}\right)\right] dR\, dQ$$

$$= 0 \tag{22}$$

Where:

$$w = w_R.w_Q.w_S \tag{23}$$

$$w_1 = w_R.w_Q \tag{24}$$

$$N_x = N_{x1} + N_{xs} \tag{25}$$

For Equation (22) to be true, its integrand must be zero. That is:

$$\left(\frac{\partial^4 w_1}{\partial R^4} + \frac{2}{\beta^2}\cdot\frac{\partial^4 w_1}{\partial R^2 \partial Q^2} + \frac{1}{\beta^4}\cdot\frac{\partial^4 w_1}{\partial Q^4} - \frac{N_{x1}a^4}{gD^*}\cdot\frac{\partial^2 w_1}{\partial R^2}\right)w_S$$
$$+ \frac{w_1}{g}\left(\frac{(1-\mu)a^4}{t^4}\cdot\frac{\partial^2 w_S}{\partial S^2} - \frac{N_{xs}a^4}{D^*}\cdot\frac{\partial^2 w_S}{\partial R^2}\right) \tag{26}$$

One of the possibilities of Equation (26) to be true is for the terms in each of the two brackets sum to zero. That is:

$$\frac{\partial^4 w_1}{\partial R^4} + \frac{2}{\beta^2}\cdot\frac{\partial^4 w_1}{\partial R^2 \partial Q^2} + \frac{1}{\beta^4}\cdot\frac{\partial^4 w_1}{\partial Q^4} - \frac{N_{x1}a^4}{gD^*}\cdot\frac{\partial^2 w_1}{\partial R^2} = 0 \tag{27}$$

$$\frac{(1-\mu)a^4}{t^4}\cdot\frac{\partial^2 w_S}{\partial S^2} - \frac{N_{xs}a^4}{D^*}\cdot\frac{\partial^2 w_S}{\partial R^2} = 0 \tag{28}$$

Given that;

$$w = w_1.w_S \tag{29}$$

Putting the Equation (29) into (27) and solve to get the exact deflection function in polynomial as:

$$w = \Delta_0\,(a_0 + \ a_1 R + a_2 R^2 + a_3 R^3 + \ a_4 R^4).(b_0 + \ b_1 Q + \ b_2 Q^2 + b_3 Q^3 + b_4 Q^4) \tag{30}$$

Where:

$$w = A_1.h \tag{31}$$
$$w_S = \Delta_0 + \Delta_1 S \tag{32}$$

And,

$$w_S = \Delta_0 \tag{33}$$

Substituting Equation (30) into the re-arranged Equation (6) and simplifying the outcome gives:

$$\theta_{sx} = \frac{c}{a}.\Delta_0.(1\ \ 2R\ \ 3R^2\ \ 4R^3)\begin{bmatrix}a_1\\a_2\\a_3\\a_4\end{bmatrix}.(1\ \ Q\ \ Q^2\ \ Q^3\ \ Q^4)\begin{bmatrix}b_0\\b_1\\b_2\\b_3\\b_4\end{bmatrix} \tag{34}$$

Similarly;

$$\theta_{sy} = \frac{c}{a\beta}.\Delta_0.(1\ \ R\ \ R^2\ \ R^3\ \ R^4)\begin{bmatrix}a_0\\a_1\\a_2\\a_3\\a_4\end{bmatrix}.(1\ \ 2Q\ \ 3Q^2\ \ 4Q^3)\begin{bmatrix}b_1\\b_2\\b_3\\b_4\end{bmatrix} \tag{35}$$

In symbolic forms, Equations (34) and (35) are:

$$\theta_{sx} = \frac{A_{2R}}{a}.\frac{\partial h}{\partial R} \tag{36}$$
$$\theta_{sy} = \frac{A_{2Q}}{a\beta}.\frac{\partial h}{\partial Q} \tag{37}$$

Given that: h is the shape function of the plate, A_1 is the coefficient of deflection A_2 and A_3 are the coefficients of shear deformation in x axis and y axis respectively.

　　Where:

　　The coefficient of deflection of the plate is given as;

$$A_1 = \Delta_0 \begin{bmatrix}a_0\\a_1\\a_2\\a_3\\a_4\end{bmatrix}.\begin{bmatrix}b_0\\b_1\\b_2\\b_3\\b_4\end{bmatrix} \tag{38}$$

　　The plates shape function becomes;

$$h = [1\ \ R\ \ R^2\ \ R^3\ \ R^4].[1\ \ Q\ \ Q^2\ \ Q^3\ \ Q^4] \tag{39}$$

2.3. Direct Governing Equation

By substituting Equations (31), (36) and (37) into the Energy equation obtained in Equation (17) and differentiating with respect to deflection coefficient (A_1), the direct governing equation of the plate is given as:

$$\frac{\partial \Pi}{\partial A_1} = 6(1-2\mu)\left(\frac{a}{t}\right)^2\left([A_1 + M_2 A_1].k_R + \frac{1}{\beta^2}.[A_1 + M_3 A_1].k_Q\right) - \frac{N_x a^2 A_1}{D^*}.k_R = 0 \tag{40}$$

This gives:

$$\frac{a^2 N_x}{Et^3} = \frac{(1+\mu)}{2}\left(\frac{a}{t}\right)^2 \left([1+M_2] + \frac{1}{\beta^2}\cdot[1+M_3]\cdot\frac{k_Q}{k_R}\right) \tag{41}$$

Given that D^* is the Rigidity for 3-D thick plate, let

$$D^* = D\frac{(1-\mu)}{(1-2\mu)}$$

Where:

$$k_{RR} = \int_0^1\int_0^1\left(\frac{\partial^2 h}{\partial R^2}\right)^2 dRdQ: \ k_{RQ} = \int_0^1\int_0^1\left(\frac{\partial^2 h}{\partial R\partial Q}\right)^2 dRdQ; \ k_{QQ} = \int_0^1\int_0^1\left(\frac{\partial^2 h}{\partial Q^2}\right)^2 dRdQ \tag{42}$$

$$k_R = \int_0^1\int_0^1\left(\frac{\partial h}{\partial R}\right)^2 dRdQ; \ k_Q = \int_0^1\int_0^1\left(\frac{\partial h}{\partial Q}\right)^2 dRdQ \tag{43}$$

Minimizing Equation (17) with respect to A_{2R} and A_{2Q} after substituting Equations (31), (36) and (37) into it gives:

$$A_{2R} = M_2 A_1 \tag{44}$$
$$A_{2Q} = M_3 A_1 \tag{45}$$

Equations 44 and 45 is solved simultaneously to get:

$$M_2 = \frac{(m_{12}m_{23} - m_{13}m_{22})}{(m_{12}m_{12} - m_{11}c_{22})}; \ M_3 = \frac{(m_{12}m_{13} - m_{11}m_{23})}{(m_{12}m_{12} - m_{11}m_{22})} \tag{46}$$

$$m_{11} = (1-\mu)k_{RR} + \frac{1}{2\beta^2}(1-2\mu)k_{RQ} + 6(1-2\mu)\left(\frac{a}{t}\right)^2 k_R \tag{47}$$

$$m_{22} = \frac{(1-\mu)}{\beta^4}k_{QQ} + \frac{1}{2\beta^2}(1-2\mu)k_{RQ} + \frac{6}{\beta^2}(1-2\mu)\left(\frac{a}{t}\right)^2 k_Q \tag{48}$$

$$m_{12} = m_{21} = \frac{1}{2\beta^2}k_{RQ}; \ m_{13} = -6(1-2\mu)\left(\frac{a}{t}\right)^2 k_R; \ m_{23} = m_{32} = -\frac{6}{\beta^2}(1-2\mu)\left(\frac{a}{t}\right)^2 k_Q \tag{49}$$

2.4. Numerical Analysis

A problem of a rectangular thick plate that is clamped at one edge and the other three edges simply supported (CSSS) under uniaxial compressive load is presented. The displacement function as presented in the Equation (30), (34) and (30) was applied through variation to obtain the solution of the critical buckling load in the plate by subjecting it to CSSS boundary condition.

The boundary conditions of the CSSS rectangular plate presented in the Figure 1 are as follows:

At $R = Q = 0$; deflection $(w) = 0$ $\hspace{3cm}$ (50)

At $R = 0$, bending moment $\left(\frac{d^2w}{dR^2}\right) = 0$; $Q = 0$, slope $\left(\frac{dw}{dQ}\right) = 0$ $\hspace{1cm}$ (51)

At $R = Q = 1$, deflection $(w) = 0$; $\hspace{3cm}$ (52)

At $R = Q = 1$, bending moment $\left(\frac{d^2w}{dR^2} \ and \ \frac{d^2w}{dR^2}\right) = 0$ $\hspace{2cm}$ (53)

Substituting Equation (50) to (53) into the derivatives of w and solving gave the characteristic equation gives the following constants:

$$a_0 = 0; \ a_1 = a_4; \ a_2 = 0; \ a_3 = -2a_4 \ and \tag{54}$$
$$b_0 = 0; \ b_1 = 0; \ b_2 = 1.5b_4; \ b_3 = -2.5b_4 \tag{55}$$

Substituting the constants of Equation (54) and (55) into Equation (30) gives;

$$w = (a_4 R - 2a_4 R^3 + a_4 R^4) \times (1.5b_4 Q^2 - 2.5b_4 Q^3 + b_4 Q^4) \tag{56}$$

Simplifying Equation (56) which satisfying the boundary conditions of Equation (50) to (53) gives:

$$w = a_4 \times b_4 (R - 2R^3 + R^4) \times (1.5Q^2 - 2.5Q^3 + Q^4) \tag{57}$$

Let the amplitude,

$$A_1 = a_4 \times b_4 \tag{61}$$

And;

$$h = (R - 2R^3 + R^4) \times (1.5Q^2 - 2.5Q^3 + Q^4) \tag{62}$$

Thus, the polynomial deflection functions after satisfying the boundary conditions is:

$$w = (R - 2R^3 + R^4) \times (1.5Q^2 - 2.5Q^3 + Q^4).A_1 \tag{63}$$

Using Equation (42) and (43) after putting Equation (62) into it, a numerical values of the stiffness CSSS rectangular plate were obtained as presented in Table 1.

Table 1: The polynomial and trigonometric stiffness coefficients of deflection function of the CSFS plate

Displacement Shape Function	k_{RR}	k_{RQ}	k_{QQ}	k_R	k_Q
Present Study	0.03619	0.04163	0.08857	0.00366	0.00422
Onyeka *et al.* [28]	928.2428	1,015.280	2,057.980	94.05066	102.8692

3. RESULTS AND DISCUSSIONS

In this section, Equation 30 showed the expression of deflection function which was derived to get the formulae for predicting the buckling load of the plate. The graphical re-presentation of the result of the critical buckling load of a rectangular plate that is clamped and simply supported at the other three edges (CSSS), as calculated is shown in the Figures 2 to 10. This result also showed the comparative stability analysis between the present work and the work of Onyeka *et al.* [28] for CSSS plate subjected to uniaxial compressive load at varying aspect ratio.

The values obtained in Figure 2 to 10, shows that as the values of critical buckling load increase, the span- thickness ratio increases. This reveals that as the in-plane load on the plate increase and approaches the critical buckling, the failure in a plate structure is a bound to occur; this means that a decrease in the thickness of the plate, increases the chance of failure in a plate structure. Hence, failure tendency in the plate structure can be mitigated by increasing its thickness. It is also observed in the figures that as the length to breadth ratio (aspect ratio) of the plate increases, the value of critical buckling load decreases while as critical buckling load increases as the length to breadth ratio increases. This implies that an increase in plate width increases the chance of failure in a plate structure. It can be deduced that as the in-plane load which will cause the plate to fail by compression increases from zero to critical buckling load, the buckling of the plate exceeds specified elastic limit thereby causing failure in the plate structure. This meant that, the load that causes the plate to deform also causes the plate material to buckle simultaneously.

Looking closely at the result of buckling load for the present study at the span to thickness ratio of 20 and beyond, it is seen that the value of critical buckling load of the plate maintained a constant value of 5.62 for square plate, 2.47 for aspect ratio of 1.5, 1.70 for aspect ratio of 2.0, 1.40 for aspect ratio of 2.5, 1.27 for aspect ratio of 3.0, 1.19 for aspect ratio of 3.5, 1.14 for aspect ratio of 4.0, 1.11 for aspect ratio of 4.5, 1.08 for aspect ratio of 5.0. This proof that the value of critical load for thin plate and thick plate (see [8]) which described the thin and moderately thick plate as the one whose span to thickness ratio is equal or less than 30.

A numerical and graphical comparison was made to show the disparities between the present study and the literature under review to show the effect of aspect ratio on the buckling load in a 3-D stability analysis of rectangular plate at varying thickness. The span to thickness ratio considered is ranged between 4 through 1500, which is obviously seen to span from the thick plate, moderately thick plate and thin plate (see [28]). The present work obtained non-dimensional result of buckling load of the plate by expressing the displacement shape function of the plate in the form of polynomial to analyze the effect of aspect ratio on the critical buckling load of the plate while the work of Onyeka *et al.* [28] was obtained by expressing the displacement shape function of the plate in the form of trigonometry to analyze the effect of aspect ratio on the critical buckling load of the plate. The aspect ratio of the plate into consideration includes; 1, 1.5, 2.0, 2.5, 3.0, 3.5, 4.0, 4.5 and 5.0. The comparison shows that the present theory using polynomial functions predicts a slightly lower value of the critical buckling load than the previous study (Onyeka *et al.* [28]) when the plate is thicker and higher value as the plate is thinner. This is quite expected because the trigonometric function gives higher value of the stiffness coefficient than polynomial, and thus safe to use in the thick plate analysis as the variation produce an upper bound solution which will not put the structure in danger.

The percentage difference of critical buckling load between the present study and the previous study [28] for an isotropic CSSS rectangular plate at a variable aspect ratio is presented in Table 2. The highest average percentage difference is 6.098 which occurs in the square plate at span to thickness ratio of 100 to 1500, while the lowest average percentage difference is 0.526 which occur in an aspect ratio of five (5) at span to thickness ratio of 4. The average percentage difference between the two studies at aspect ratio of 1.0, 1.5, 2.0, 2.5, 3.0, 3.5, 4.0, 4.5 and 5.0 is 5.95, 3.88, 2.56, 1.78, 1.01, 0.81, 0.67 and 0.57. It is shown in the table that the degree of the percentage difference between the two studies decreases as the aspect ratio of the plate decreases. This implies that as the length of the plate widens, the credibility of the studies becoming almost the same. Furthermore, it was discovered that the values of the percentage difference between the two studies decrease as the span to thickness ratio of the plate decreases. This implies that as the plate gets thinner, the studies differs more and becomes almost the same for thick plates. This could mean that the theories used by the present and previous studies are suitable for thick plate analysis. This, however, shows the high level of convergence between the theories and approaches. It also implies a high level of accuracy of the derived relationships and thus proof reliability of the process in the stability analysis of rectangular plate of any category (thin, moderately thick and thick plate). Finally, the overall

average percentage differences between the two studies using different functions recorded are 2.06%. These differences being less than 5% are quite acceptable in statistical analysis, as it will not put the structure into danger. This shows that at about 98% both approaches are the same under the same boundary condition and can be applied with confidence in the stability analysis of any type of rectangular plate.
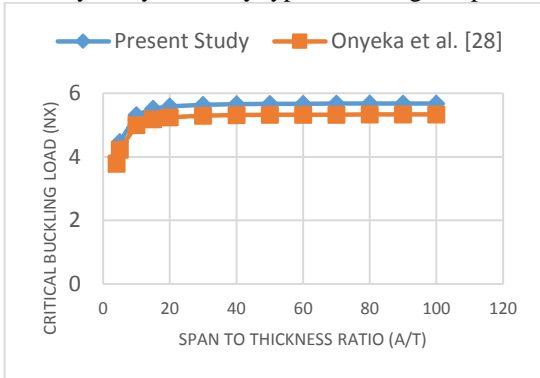

Figure 2: Graph of Critical buckling load (N_x) versus span to thickness ratio of a rectangular plate at aspect ratio of 1.0
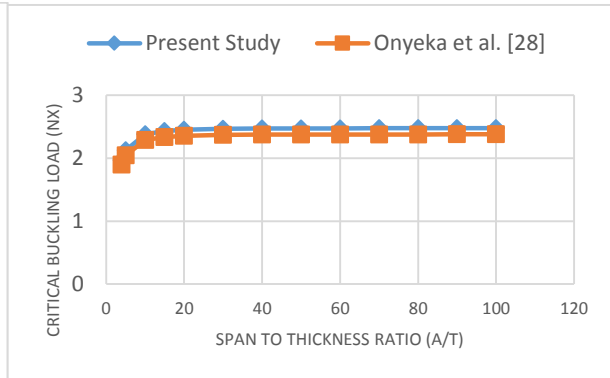

Figure 3: Graph of Critical buckling load (N_x) versus span to thickness ratio of a rectangular plate at aspect ratio of 1.5
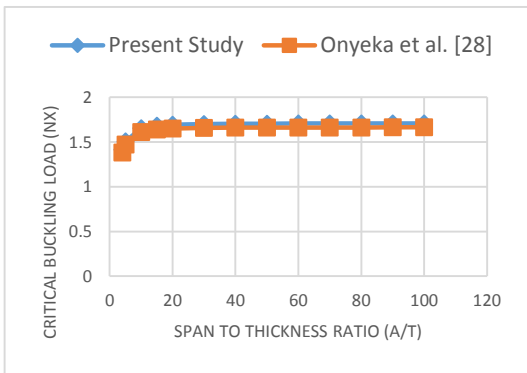

Figure 4: Graph of Critical buckling load (N_x) versus span to thickness ratio of a rectangular plate at aspect ratio of 2.0
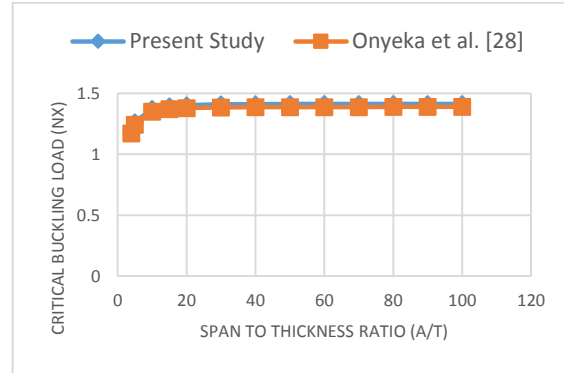

Figure 5: Graph of Critical buckling load (N_x) versus span to thickness ratio of a rectangular plate at aspect ratio of 2.5
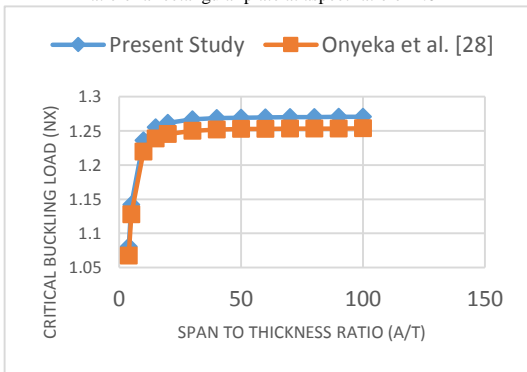

Figure 6: Graph of Critical buckling load (N_x) versus span to thickness ratio of a rectangular plate at aspect ratio of 3.0

Figure 7: Graph of Critical buckling load (N_x) versus span to thickness ratio of a rectangular plate at aspect ratio of 3.5

Figure 8: Graph of Critical buckling load (N_x) versus span to thickness ratio of a rectangular plate at aspect ratio of 4.0
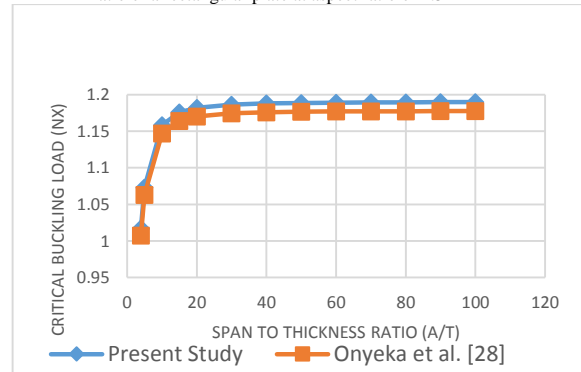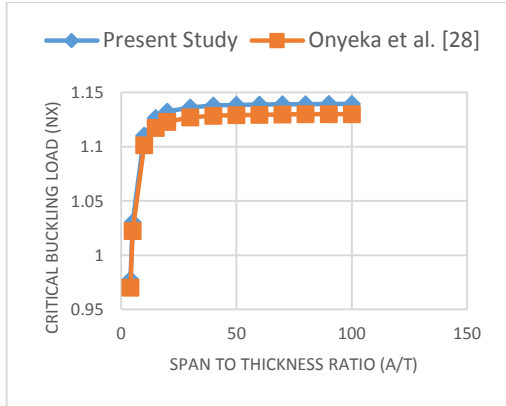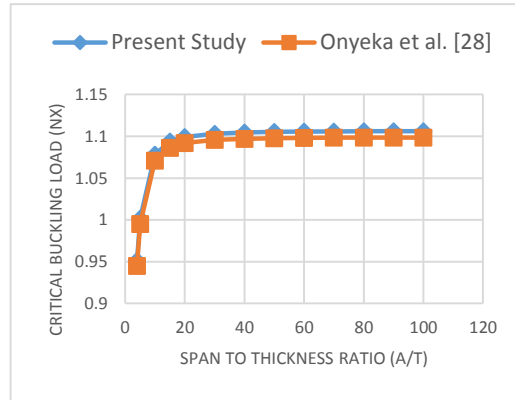

Figure 9: Graph of Critical buckling load (N_x) versus span to thickness ratio of a rectangular plate at aspect ratio of 4.5
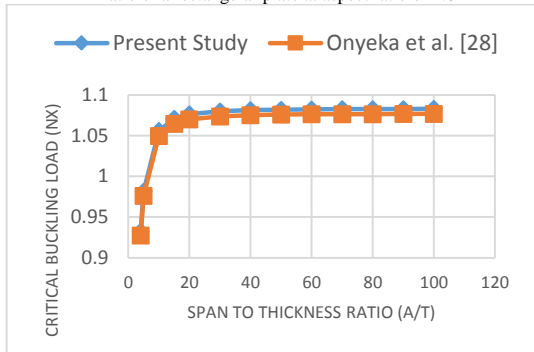

Figure 10: Graph of Critical buckling load (N_x) versus span to thickness ratio of a rectangular plate at aspect ratio of 5.0

Table 2: Percentage difference of buckling load on the CSSS rectangular plate between Present work and Onyeka *et al.* [28]

$\propto = \frac{a}{t}$	Average Percentage Difference %								
	$\beta = 1.0$	$\beta = 1.5$	$\beta = 2.0$	$\beta = 2.5$	$\beta = 3.0$	$\beta = 3.5$	$\beta = 4.0$	$\beta = 4.5$	$\beta = 5.0$
4	5.1014	3.48	2.3397	1.6429	1.2133	0.9371	0.7511	0.6207	0.5261
5	5.3839	3.6242	2.4213	1.6950	1.2501	0.9649	0.7734	0.6394	0.5422
10	5.8853	3.8569	2.5486	1.7752	1.3062	1.0073	0.8072	0.6675	0.5664
15	5.9998	3.9063	2.5749	1.7916	1.3176	1.0158	0.8141	0.6732	0.5713
20	6.0419	3.9241	2.5843	1.7974	1.3216	1.0189	0.8165	0.6752	0.5730
30	6.0726	3.9370	2.5912	1.8017	1.3246	1.0211	0.8183	0.6767	0.5743
40	6.0835	3.9416	2.5936	1.8031	1.3256	1.0219	0.8189	0.6772	0.5747
50	6.0885	3.9437	2.5947	1.8038	1.3261	1.0223	0.8192	0.6774	0.5749
60	6.0913	3.9448	2.5953	1.8042	1.3264	1.0225	0.8193	0.6776	0.5750
70	6.0929	3.9455	2.5956	1.8044	1.3265	1.0226	0.8194	0.6777	0.5751
80	6.0940	3.946	2.5959	1.8046	1.3266	1.0227	0.8195	0.6777	0.5752
90	6.0948	3.9463	2.5960	1.8047	1.3267	1.0227	0.8195	0.6777	0.5752
100	6.0953	3.9465	2.5962	1.8048	1.3267	1.0227	0.8195	0.6778	0.5752
1000	6.0975	3.9474	2.5967	1.8051	1.3269	1.0229	0.8197	0.6779	0.5753
1500	6.0975	3.9474	2.5967	1.8051	1.3269	1.0229	0.8197	0.6779	0.5753
Average % difference	5.9547	3.8825	2.5614	1.7829	1.3115	1.0112	0.8103	0.6701	0.5686
Total Average % difference	2.06								

4.   CONCLUSION

The result of this study as recorded in the percentage difference analysis showed that the 2-D refined plate theory (RPT) is only an approximate relation for buckling analysis of thick plate and when applied to the thick plate will under-predicts buckling loads as they

neglect the transverse normal stresses along the thickness axis of the plate. Thus, the polynomial and trigonometric displacement function developed in this study produces an exact solution as they emanated from a complete three-dimensional theory which is more reliable solution in the stability analysis of plates and, can be recommended for analysis of any type of rectangular plate subjected to such loading and boundary condition.

References
[1]   F. C. Onyeka, B. O. Mama, Analytical Study of Bending Characteristics of an Elastic Rectangular Plate using Direct Variational Energy Approach with Trigonometric Function, (2021) *Emerging Science Journal*. 5(6): 916-928. doi:10.28991/esj-2021-01320.
[2]   F. C. Onyeka, B. O. Mama, T. E. Okeke, Exact Three-Dimensional Stability Analysis of Plate Using a Direct Variational Energy Method, (2022) *Civil Engineering Journal*, 8 (1), 60-80. http://dx.doi.org/10.28991/CEJ-2022-08-01-05.
[3]   F.C. Onyeka, B. O. Mama, and C. D. Nwa-David, Analytical Modelling of a Three-Dimensional (3D) Rectangular Plate Using the Exact Solution Approach, (2022) *IOSR Journal of Mechanical and Civil Engineering (IOSR-JMCE),* 11(1), 10-22. doi: 10.9790/1684-1901017688.
[4]   R. D. Mindlin, Influence of Rotatory Inertia and Shear on Flexural Motions of Isotropic, Elastic Plates, (1951) *Journal of Applied Mechanics* 18(1): 31–38. doi:10.1115/1.4010217.
[5]   J.N. Reddy, *Classical Theory of Plates*, In Theory and Analysis of Elastic Plates and Shells, (2006) CRC Press. doi: 10.1201/9780849384165-7.
[6]   F.C. Onyeka, Direct Analysis of Critical Lateral Load in a Thick Rectangular Plate using Refined Plate Theory, (2019) *International Journal of Civil Engineering and Technology,* 10(5), 492-505.
[7]   F.C. Onyeka., C.D. Nwa-David, and E.E. Arinze, Structural Imposed Load Analysis of Isotropic Rectangular Plate Carrying a Uniformly Distributed Load Using Refined Shear Plate Theory, (2021) *FUOYE Journal of Engineering and Technology (FUOYEJET),* 6(4), 414-419. http://dx.doi.org/10.46792/fuoyejet.v6i4.719.
[8]   F.C. Onyeka, F.O. Okafor, H,N, Onah, Application of Exact Solution Approach in the Analysis of Thick Rectangular Plate, (2019) *International Journal of Applied Engineering Research,* 14(8), 2043-2057.
[9]   K. Chandrashekhara. Theory of plates, (2001) University Press (India) Limited.
[10] J.C. Ezeh, O.M. Ibearugbulem, L.O. Ettu, L.S. Gwarah, I.C. Onyechere, Application of Shear Deformation Theory for Analysis of CCCS and SSFS Rectangular Isotropic Thick Plates, (2018) *IOSR Journal of Mechanical and Civil Engineering (IOSR-JMCE)*, 15 (5), 33-42.
[11] F.C. Onyeka, O.M. Ibearugbulem, Load Analysis and Bending Solutions of Rectangular Thick Plate, (2020) *International Journal on Emerging Technologies*, *11*(3): 1103–1110.
[12] O.M. Ibearugbulem, S.I. Ebirim, U.C. Anya, L.O. Ettu, Application of Alternative II Theory to Vibration and Stability Analysis of Thick Rectangular Plates (Isotropic and Orthotropic), (2020) *Nigerian Journal of Technology (NIJOTECH).* 39(1), 52 – 62. http://dx.doi.org/10.4314/njt.v39i1.6
[13] D.O. Onwuka, S.E. Iwuoha, Elastic instability analysis of biaxially compressed flat rectangular isotropic all-round clamped (CCCC) plates, (2017) MOJ Civil Eng. 2(2):52–56. DOI: 10.15406/mojce.2017.02.00027
[14] S.P. Timoshenko, J.M. Gere, W. Prager, Theory of Elastic Stability, Second Edition, (1962) Journal of Applied Mechanics (2nd ed., Vol. 29, Issue 1). McGraw-Hill Books Company. doi:10.1115/1.3636481.
[15] J.N. Reddy, Classical Theory of Plates. In Theory and Analysis of Elastic Plates and Shells (2006) CRC press. doi:10.1201/9780849384165-7.
[16] G. Kirchhoff, Über das Gleichgewicht und die Bewegung einer elastischen Scheibe, (1850) *Journal Fur Die Reine Und Angewandte Mathematik*, (40), 51–88. doi:10.1515/crll.1850.40.51.
[17] E. Reissner, The Effect of Transverse Shear Deformation on the Bending of Elastic Plates, (1945) *Journal of Applied Mechanics*, 12(2), A69–A77. doi:10.1115/1.4009435.
[18] F.C. Onyeka, E.T. Okeke, J. Wasiu, Strain–Displacement Expressions and their Effect on the Deflection and Strength of Plate, (2020) *Advances in Science, Technology and Engineering Systems Journal* 5(5), 401-413. https://dx.doi.org/10.25046/aj050551
[19] N.G. Iyengar, Structural Stability of Columns and Plates, (1988) New York: Ellis Horwood Limited.
[20] J.C Ezeh, I.C. Onyechere, O.M. Ibearugbulem, U.C. Anya, L. Anyaogu, Buckling Analysis of Thick Rectangular Flat SSSS Plates using Polynomial Displacement Functions, (2018) *International Journal of Scientific & Engineering Research,* 9(9): 387-392.
[21] F.C. Onyeka, Critical Lateral Load Analysis of Rectangular Plate Considering Shear Deformation Effect, (2020) *Global Journal of Civil Engineering, 1,* 16–27. doi:10.37516/global.j.civ.eng.2020.0121.
[22] O.M. Ibearugbulem, V.T. Ibeabuchi, and K.O. Njoku, Buckling analysis of SSSS stiffened rectangular isotropic plates using work principle approach, (2014) *International Journal of Innovative Research & Development,* 3(11), 169-176.
[23] A.S. Sayyad, Y.M Ghugal, Buckling analysis of thick isotropic plates by using Exponential Shear Deformation Theory, (2012) *Applied and Computational Mechanics*, 6, 185–196.
[24] S.M. Gunjal, R.B. Hajare, A.S. Sayyad, M.D. Ghodle, Buckling analysis of thick plates using refined trigonometric shear deformation theory, (2015) *Journal of Materials and Engineering Structures* 2. 159–167.
[25] Shufrin and M. Eisenberger, Stability and vibration of shear deformable plates - First order and higher order analyses, (2005) *International Journal of Solids and Structures,* 42(3-4): 1225–1251.
[26] A.M. Vareki, B.N. Neya, J.V. Amiri, 3-D Elasticity Buckling Solution for Simply Supported Thick Rectangular Plates using Displacement Potential Functions, (2016) *Applied Mathematical Modelling*, 40: 5717–5730.
[27] F.C. Onyeka, B.O. Mama, J. Wasiu, An Analytical 3-D Modeling Technique of Non-Linear Buckling Behavior of an Axially Compressed Rectangular Plate, (2022) *International Research Journal of Innovations in Engineering and Technology – IRJIET"* 6(1), 91-101. doi https://doi.org/10.47001/IRJIET/2022.601017.
[28] F.C. Onyeka, F.O Okafor, H.N. Onah, Application of a New Trigonometric Theory in the Buckling Analysis of Three-Dimensional Thick Plate, (2021) *International Journal on Emerging Technologies*, 12(1): 228-240.